Available online at www.sciencedirect.com
ScienceDirect
Thermochimica Acta 459 (2007) 64–72
thermochimica acta
www.elsevier.com/locate/tca

Thermal analysis of halotrichites

Ashley J. Locke, Wayde N. Martens, Ray L. Frost *

Inorganic Materials Research Program, School of Physical and Chemical Sciences, Queensland University of Technology, GPO Box 2434, Brisbane, Queensland 4001, Australia

Received 15 February 2007; received in revised form 18 April 2007; accepted 20 April 2007
Available online 29 April 2007

Abstract

Four halotrichites from different origins were analysed by thermogravimetric and differential thermogravimetric analysis. The halotrichites were analysed by powder X-ray diffraction and were phase pure. The chemical composition was analysed using EDX techniques. The formula of the halotrichite minerals were determined as halotrichite $(Fe_{0.75}^{2+},Mg_{0.25})SO_4{\cdot}Al_2(SO_4)_3{\cdot}22H_2O$, apjohnite $(Mn_{0.64}^{2+},Mg_{0.28},Zn_{0.08})SO_4{\cdot}Al_2(SO_4)_3{\cdot}22H_2O$, pickeringite $(Fe_{0.22}^{2+},Mg_{0.78})SO_4{\cdot}Al_2(SO_4)_3{\cdot}22H_2O$, wupatkiite as $(Co_{0.45},Fe_{0.55}^{2+})SO_4{\cdot}Al_2(SO_4)_3{\cdot}22H_2O$. Three low temperature decomposition steps (a) between 0 and 44 °C, 50 and 76 °C, 72 and 88 °C were attributed to dehydration. An additional dehydration step at around 317–330 °C was confirmed by in situ mass spectrometry. The higher temperature decomposition steps between 516 and 738 °C are attributed to the decomposition of sulphate to sulphur dioxide and oxygen as confirmed by mass spectrometry. A comparison of the thermal decomposition of jarosites is made.

Keywords: Evaporite; Jarosite; Halotrichite; Sulphate; Raman spectroscopy

1. Introduction

The minerals in the halotrichite group have been known for an extended period of time [1–6]. The minerals are monoclinic sulphates of general formula $AB_2(SO_4)_4{\cdot}22H_2O$ where A is Mg, Mn^{2+}, Fe^{2+}, Ni, Zn and some combination of these cations and B may be Al, Cr^{3+} or Fe^{3+}. These minerals are also known as pseudoalums. Metals such as manganese, ferrous iron, cobalt, zinc and magnesium will form double sulphates. These sulphates are related to the halotrichites mineral series. These alums are not isomorphous with the univalent alums. Typically the end member formulae are $MgSO_4{\cdot}Al_2(SO_4)_3{\cdot}22H_2O$ (pickeringite) or $FeSO_4{\cdot}Al_2(SO_4)_3{\cdot}22H_2O$ (halotrichite), but other M^{2+} cations substitute and solid solutions in the series are extensive. These minerals are referred to as the pseudo-alums [7–9], and are often found in nature as post-mining phases [7–9]. Apjohnite is the manganese pseudo-alum. Wupatkiite is the cobalt analogue, which may have some other divalent metal substitution for the cobalt cation [10]. The minerals are all isomorphous and crystallise in the monoclinic space group $P2_1/c$ [11]. In the structure of the pseudo-alums, four crystallographically independent sulphate ions are present [11–15]. One acts as a unidentate ligand to the M^{2+} ion, and the other three are involved in complex hydrogen bond arrays involving coordinated water molecules to both cations and to the lattice water molecules [13].

The thermal decomposition of jarosites has been studied for some considerable time [16–20]. There have been many studies on related minerals such as the Fe(II) and Fe(III) sulphate minerals [21–26]. Interest in such minerals and their thermal stability rests with the possible identification of these minerals and related dehydrated paragenetically related mineral on planets and on Mars. The existence of these minerals on planets would give a positive indication of the existence or at least pre-existence of water. Further such minerals are formed through crystallisation from solutions. It has been stated that the thermal decomposition of jarosite begins at 400 °C with the loss of water [27]. The process is apparently kinetically driven. Water loss can occur at low temperatures over extended periods of time [27]. It is probable that in nature low temperature environments would result in the decomposition of jarosite. The products of the decomposition depend upon the jarosite be it K, Na or Pb, etc. but normally goethite and hematite are formed together with soluble sulphates [28]. Recently thermogravimetric analysis has been applied to some complex mineral systems and it is considered that TG–MS

* Corresponding author. Tel.: +61 7 3138 2407; fax: +61 7 3138 1804.
E-mail address: r.frost@qut.edu.au (R.L. Frost).

0040-6031/$ – see front matter © 2007 Elsevier B.V. All rights reserved.
doi:10.1016/j.tca.2007.04.015

analyses may also be applicable to the jarosite minerals [29–34]. Raman spectroscopy has proven very useful for the study of minerals [35–37]. Indeed Raman spectroscopy has proven most useful for the study of diagentically related minerals as often occurs with carbonate minerals [38–42]. Some previous studies have been undertaken by the authors using Raman spectroscopy to study complex secondary minerals formed by crystallisation from concentrated sulphate solutions [43]. To the best of the authors knowledge no thermoanalytical studies of halotrichites have been undertaken; although differential thermal analysis of some related minerals has been published [18,44–46]. In this work we report the thermogravimetric analysis of a selection of natural halotrichites.

2. Experimental

2.1. Minerals

The halotrichite minerals used in this work were supplied by the Mineralogical Research Company and The Museum of South Australia. The minerals were analysed by X-ray diffraction for phase purity and by electron probe using energy dispersive techniques for quantitative chemical composition. Table 1 lists the minerals their origin and composition as determined by EDX. The values are an average of not less than five measurements.

2.2. SEM and EDX

Mineral samples were coated with a thin layer of evaporated carbon and secondary electron images were obtained using a scanning electron microscope (FEI Quanta 200 SEM, FEI Company, Hillsboro, Oregon, USA). For X-ray microanalysis (EDX), three samples were embedded in Araldite resin and polished with diamond paste on Lamplan 450 polishing cloth using water as a lubricant. The samples were coated with a thin layer of evaporated carbon for conduction and examined in a JEOL 840A analytical SEM (JEOL Ltd., Tokyo, Japan) at 25 kV accelerating voltage. Preliminary analyses of the natural halotrichite mineral samples were carried out on the FEI Quanta SEM using an EDAX X-ray microanalyser, and microanalyses of the clusters of fine crystals were carried out using a full standards quantitative procedure on the JEOL 840 SEM using a JEOL-2300 energy-dispersive X-ray microanalysis system (JEOL Ltd., Tokyo, Japan). Oxygen was not measured directly but was calculated using assumed stoichiometry of the other elements analysed. Table 1 is in at.%. The total at.% is added and the subtracted from 100.0% to obtain the oxygen at.%.

2.3. X-ray diffraction

XRD analyses were performed on a PANalytical X'Pert PRO® X-ray diffractometer (radius: 240.0 mm). Incident X-ray radiation was produced from a line focused PW3373/10 Cu X-ray tube, operating at 45 kV and 35 mA. The incident beam passed through a 0.04 rad, Soller slit, a 1/2° divergence slit, a 15 mm fixed mask and a 1° fixed anti scatter slit. After interaction with the sample, the diffracted beam was detected by an X'Celerator RTMS detector fitted to a graphite post-diffraction monochrometer. The detector was set in scanning mode, with an active length of 2.022 mm. Samples were analysed utilising Bragg–Brentano geometry over a range of 3–75° 2θ with a step size of 0.02° 2θ, with each step measured for 200 s.

2.4. Thermal analysis

Thermal decomposition of the halotrichites was carried out in a TA® Instruments incorporated high-resolution thermogravimetric analyzer (series Q500) in a flowing nitrogen atmosphere (60 cm^3/min). Approximately 35 mg of sample underwent thermal analysis, with a heating rate of 5 °C/min, resolution of 6, to 1000 °C. With the quasi-isothermal, quasi-isobaric heating program of the instrument the furnace temperature was regulated precisely to provide a uniform rate of decomposition in the main decomposition stage.

The TGA instrument was coupled to a Balzers (Pfeiffer) mass spectrometer for gas analysis. Only water vapour, carbon dioxide and oxygen were analysed. In the MS figures, e.g. Fig. 9, a background of broad peaks may be observed. This background occurs for all the ion current curves. The background becomes more prominent as the scale expansion is increased. It is considered that this background may be due to the loss of chemicals

Table 1
EDX analysis of four minerals of the halotrichite group

Atom	Apjohnite [Tariano, Italy] (average ± 0.05 at.%)	Halotrichite [Corral Hollow, California, USA] (average ± 0.05 at.%)	Pickeringite [San Bernadino, California] (average ± 0.05 at.%)	Wupatkiite [Cloncurry, Queensland, Australia] (average ± 0.05 at.%)
O	64.34	82.26	69.22	71.88
Mg	1.74	0.55	2.87	0.00
Al	9.09	4.68	7.29	6.66
S	22.97	10.45	19.96	18.19
Mn	1.39	0.00	0.00	0.00
Zn	0.47	0.00	0.00	0.00
As	0.00	0.00	0.00	0.00
Fe	0.00	2.06	0.66	1.81
Co	0.00	0.00	0.00	1.46
Total	100.0	100.0	100.0	100.0

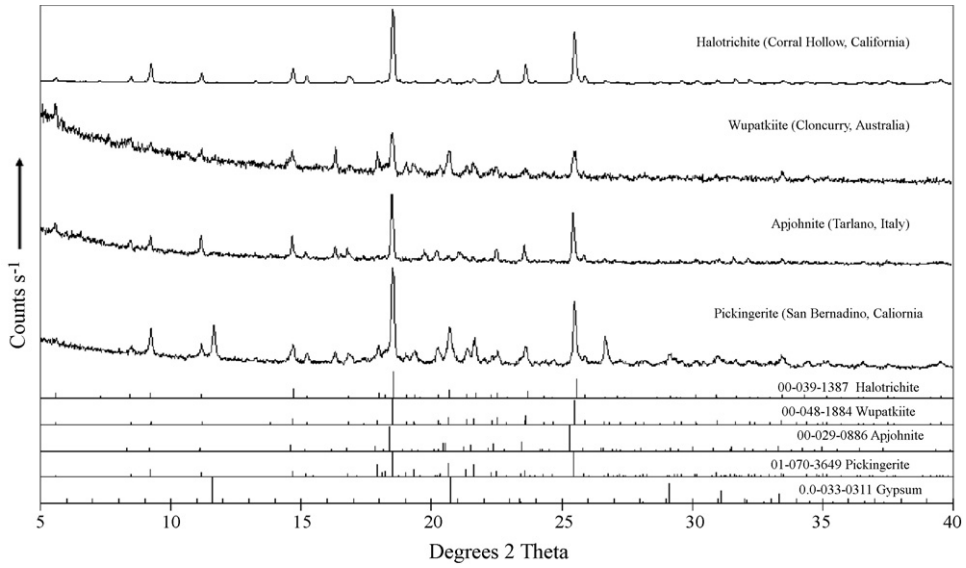

Fig. 1. XRD patterns of the four natural halotrichites and the standard reference minerals.

which have deposited in the capillary which connects the TA instrument to the MS.

3. Results and discussion

3.1. X-ray diffraction and EDX analysis

The powder X-ray diffraction patterns of the four selected minerals halotrichite, apjohnite, pickeringite and wupatkiite together with standard XRD patterns are shown in Fig. 1. The XRD patterns of the minerals show identical patterns to the standards. The XRD pattern of the pickeringite mineral shows an impurity of gypsum together with a second unknown impurity which may be jarosite.

EDX analyses are reported in Table 1. The halotrichite corresponds to an formula $(Fe_{0.75}^{2+},Mg_{0.25})SO_4{\cdot}Al_2(SO_4)_3{\cdot}22H_2O$. The EDX analysis if the apjohnite from Italy shows the presence of not only Zn and Mg but some Mn is observed as well. The formula of the apjohnite based upon the data in Table 2 is $(Mn_{0.39}^{2+},Mg_{0.48},Zn_{0.13})SO_4{\cdot}Al_2(SO_4)_3{\cdot}22H_2O$. The pickeringite EDX analyses show the presence of both Mg and Fe^{2+}. The formula of the pickeringite is therefore given as $(Fe_{0.22}^{2+},Mg_{0.78})SO_4{\cdot}Al_2(SO_4)_3{\cdot}22H_2O$. The analysis of the wupatkiite from Cloncurry, Queensland, Australia is $(Fe_{0.55}^{2+},Co_{0.45})SO_4{\cdot}Al_2(SO_4)_3{\cdot}22H_2O$.

3.2. Thermogravimetric analysis and mass spectrometric analysis

The summary of the thermogravimetric and differential thermogravimetric analyses are reported in Table 2.

3.2.1. Apjohnite

The thermogravimetric and differential thermogravimetric analysis of apjohnite are shown in Fig. 2. The associated mass spectrometric analysis is reported in Fig. 3. Six major thermal decomposition steps are observed.

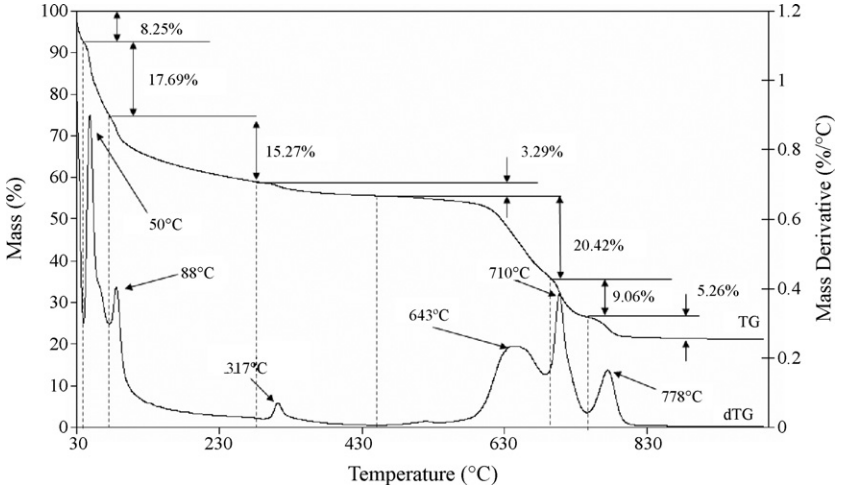

Fig. 2. TG and DTG of apjohnite.

Table 2
Halotrichite thermogravimetric analysis summary

Decomposition stage	Mineral							
	Halotrichite		Apjohnite		Pickeringite		Wupatkiite	
1st	42 °C	14.28%	31 °C	8.25%	44 °C	19.45%	51 °C	17.10%
2nd	53 °C	9.20%	50 °C	17.69%	83 °C	20.35%	76 °C	10.49%
3rd	72 °C	18.91%	88 °C	15.27%			180 °C	7.55%
4th	330 °C	3.18%	317 °C	3.29%			317 °C	11.30%
5th	546 °C	1.69%			516 °C	4.37%		
6th	625 °C	19.03%	643 °C	20.42%	631 °C	8.46%	612 °C	22.69%
7th	697 °C	7.72%	710 °C	9.06%	663 °C	5.73%	640 °C	4.55%
8th	738 °C	7.21%	778 °C	5.26%	730 °C	10.46%		

Steps 1, 2 and 3 temperature 50, 88 and 317 °C

$$(Mn_{0.39}{}^{2+}, Mg_{0.48}, Zn_{0.13})SO_4{\cdot}Al_2(SO_4)_3{\cdot}22H_2O \rightarrow (Mn_{0.39}{}^{2+}, Mg_{0.48}, Zn_{0.13})SO_4{\cdot}Al_2(SO_4)_3 + 22H_2O$$

These steps represent the loss of water and are confirmed by the ion current curves for H_2O and OH (Fig. 3). The maxima for the ion current curves for OH and H_2O are observed at 50 and 88 °C. The low temperature mass loss is due to adsorbed water [47]. The mass loss in the 50–88 °C is attributed to weakly hydrogen bonded water. The mass loss at 50 °C is 17.69% and at 88 °C is 15.2%. There is an initial mass loss up to 50 °C of 8.25% which is also attributed to the water mass loss. A small mass loss of 3.29% at 317 °C is observed. Some water molecules are retained to significantly high temperatures, perhaps because the water is trapped inside the apjohnite structure. Based upon the formula above the total theoretical mass loss is 44.95%. The total mass loss of the decomposition steps attributed to water loss is 44.50%. The theoretical and experimental mass losses are in excellent agreement. A small mass loss of <0.5% at 500 °C is observed in Fig. 2. This mass loss is attributed to the presence of a trace of jarosite in the natural mineral.

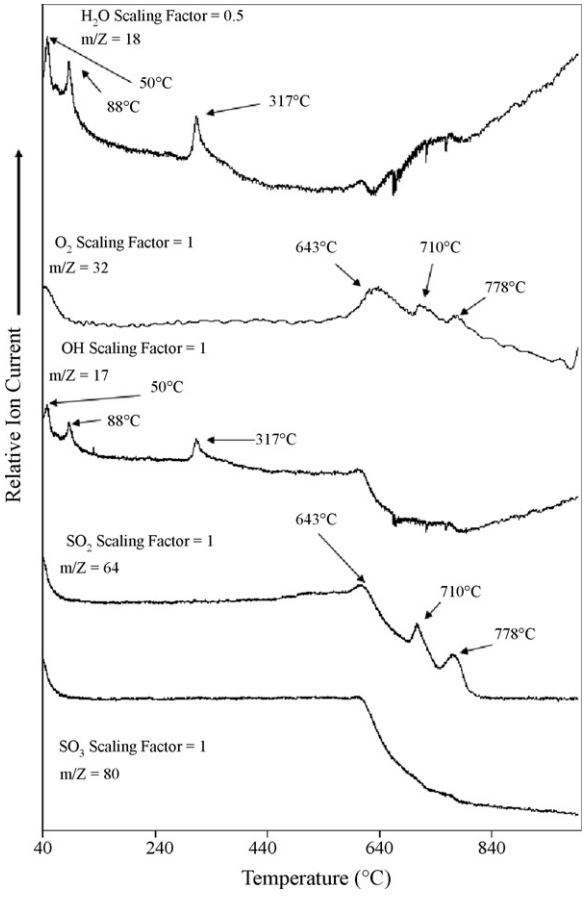

Fig. 3. Evolved gas analysis for apjohnite.

Steps 4, 5 and 6 temperatures of 643, 710 and 778 °C.

The thermal decomposition steps at 643, 710 and 778 °C are attributed to the decomposition of the sulphate anions in the apjohnite. Such decomposition is confirmed by the ion current curves of SO_2 where maxima at 643, 710 and 778 °C are observed. Similar maxima are observed in the ion current curves of oxygen. The following decomposition is proposed

$$(Mn_{0.64}{}^{2+}, Mg_{0.28}, Zn_{0.08})SO_4{\cdot}Al_2(SO_4)_3 \rightarrow Al_2O_3 + 0.64MnO + 0.28MgO + 0.08ZnO + 4SO_3$$

and

$$4SO_3 \rightarrow 4SO_2 + \tfrac{1}{2}O_2$$

The calculated mass loss based upon the formula for apjohnite above is 36.3% which compares well with the measured mass loss of 34.74%.

3.2.2. Halotrichite

The thermogravimetric and differential thermogravimetric analysis of halotrichite are shown in Fig. 4. The associated mass spectrometric analysis is reported in Fig. 5. Seven major thermal decomposition steps are observed.

Steps 1, 2, 3 and 4 temperature 53, 72 and 330 °C.

A mass loss of 14.28% is observed at quite low temperatures around or up to 42 °C. A further mass loss of 9.20% occurs at 53 °C and 18.91% up to 300 °C. A small mass loss of 3.18% is observed at 330 °C. Each of these thermal decomposition steps is attributed to dehydration of the halotrichite. The ion current curves for halotrichite of H_2O and OH units show maxima at 72 and 330 °C. Using the formula.

$(Fe_{0.75}{}^{2+},Mg_{0.25})SO_4{\cdot}Al_2(SO_4)_3{\cdot}22H_2O$ the total theoretical mass loss for water is 44.90%. The total experimental mass loss is 45.57% which is in good agreement. The water mass loss

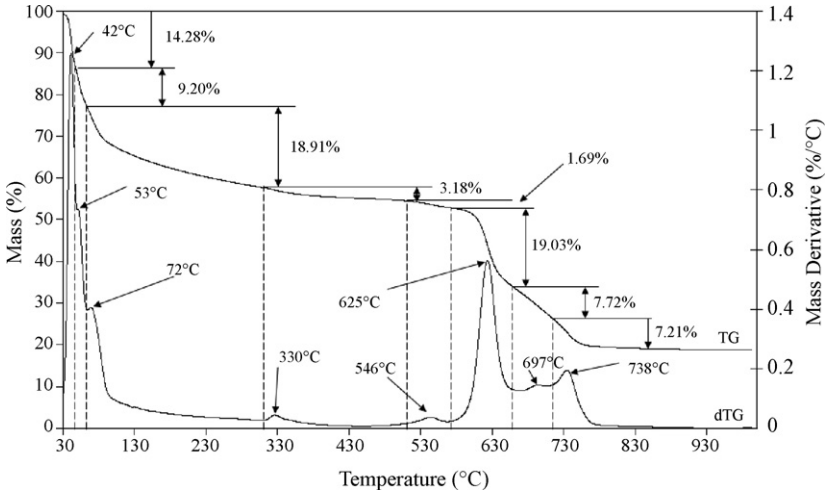

Fig. 4. TG and DTG of halotrichite.

steps appear to be at slightly lower temperatures for halotrichite in comparison to that of apjohnite.

Steps 4, 5, 6, 7 and 8 temperatures of 546, 625, 697 and 738 °C.

Four thermal decomposition steps are observed for halotrichite of the above formula at 546, 625, 697 and 738 °C. Each of these steps is assigned to the decomposition of sulphate anions, the formation of the metal oxides and the evolution of SO_2 and O_2. The mass losses at these temperatures are 1.69, 19.03, 7.72 and 7.21% making a total of mass loss of 35.65%. The theoretical mass loss calculated using the above formula is 36.29%. The measured mass loss is in agreement with the theoretical mass loss. This agreement confirms the formula of halotrichite. If the formula was different then the numbers would not be in such close agreement. These decomposition steps are confirmed by the ion current curves of the evolved gases SO_2 and O_2 where ion current maxima at 546, 625, 697 and 738 °C are observed. The maxima for evolved SO_3 are small but are observed at the same temperatures.

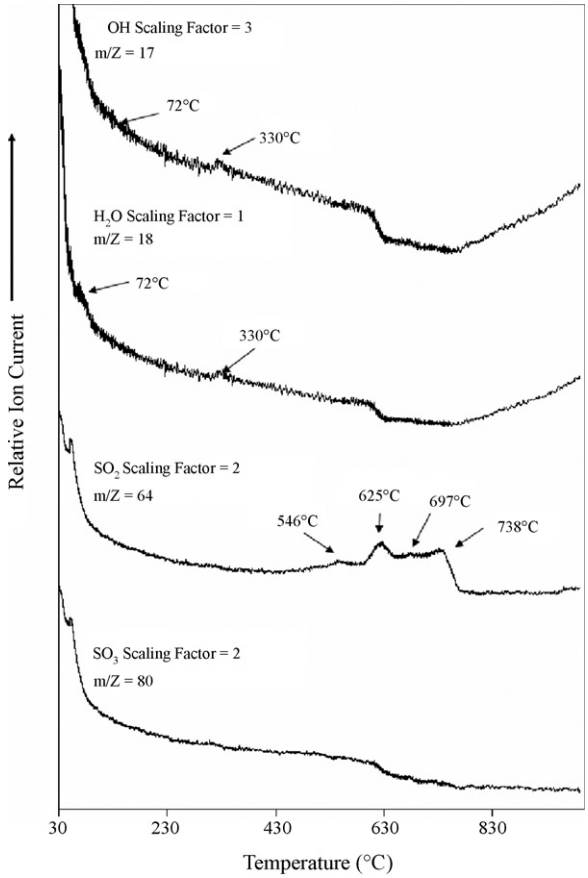

Fig. 5. Evolved gas analysis for halotrichite.

3.2.3. Pickeringite

The thermogravimetric and differential thermogravimetric analysis of pickeringite are shown in Fig. 6. The associated mass spectrometric analysis is reported in Fig. 7. Seven major thermal decomposition steps are observed.

Steps 1, 2,3 and 4 temperature 44, 83 and ~300 °C.

For pickeringite two sharp thermal decomposition steps are observed in the DTG curves at 44 and 83 °C. A very small decomposition step at around 300 °C is also observed. The mass losses at 44 and 83 °C are 19.45 and 20.35%. All these three steps are ascribed to the dehydration of the pickeringite. The ion current curves for H_2O and OH, i.e. *m*/*z* ratios of 18 and 17, respectively, show ion current maxima at 44 and 83 °C confirming the loss of water at these temperatures. By using the formula calculated from the EDX measurements of $(Fe_{0.22}{}^{2+},Mg_{0.78})SO_4{\cdot}Al_2(SO_4)_3{\cdot}22H_2O$ a total theoretical mass loss of 45.78% is estimated. The total mass loss due to dehydration is 39.80% which is in reasonable agreement with the theoretical mass loss. Any impurities in the pickingerite mineral sample such as gypsum and jarosite will affect these values. In particular their presence will be reflected in lower values that that predicted from the theoretical values.

Steps 5, 6, 7 and 8 temperatures of 516, 631, 663 and 730 °C.

Four higher temperature mass loss steps at 516, 631, 663 and 730 °C are observed for pickeringite. Mass losses of 4.37, 8.46, 5.73 and 10.46% are found for these steps making a total mass

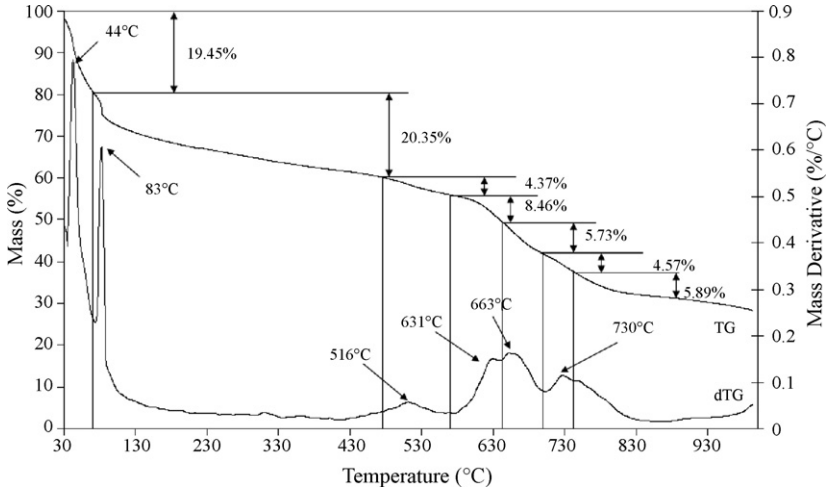

Fig. 6. TG and DTG of pickeringite.

loss of 29.02%. This value is low compared with the theoretical mass loss of total sulphate as SO_3 of 36.99%.

The total mass loss for sulphate decomposition can be calculated from the equation and the proposed formula from

$$2SO_3 \rightarrow 2SO_2 + O_2$$

The total measured mass loss is 68.82 whilst the theoretical mass loss is 82.77%. This difference may be accounted for through a number of factors (a) the mineral is a natural mineral, (b) the mineral contains low amounts of impurities and (c) the mass loss of adsorbed water is not taken into account in the total measured mass loss.

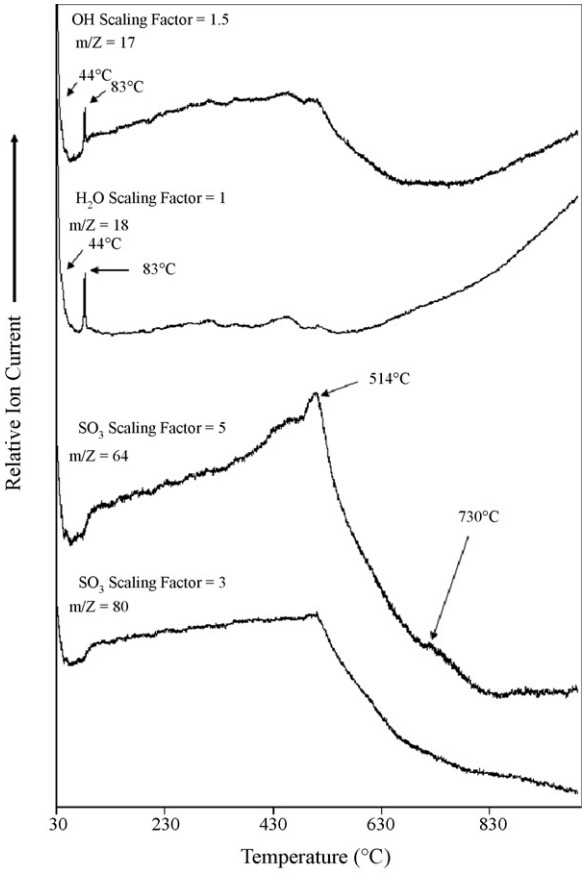

Fig. 7. Evolved gas analysis for pickeringite.

3.2.4. Wupatkiite

The thermogravimetric and differential thermogravimetric analysis of wupatkiite are shown in Fig. 8. The associated mass spectrometric analysis is reported in Fig. 9. Five major thermal decomposition steps are observed. The DTG plots for wupatkiite appear similar to that of the other halotrichites in the low temperature region but are different in the higher temperature range.

Steps 1, 2, 3 and 4 temperature 51, 76 and 317 °C.

Thermal decomposition steps at 51, 76 and 317 °C are observed with mass losses of 17.10, 10.49 and 11.30%. The ion current curves confirm the loss of water at these temperatures. There is a gradual mass loss of 7.55% over the 120–250 °C temperature range. The total mass loss attributed to dehydroxylation is 46.44%. The theoretical mass loss according to the formula $(Fe_{0.55}^{2+},Co_{0.45})SO_4{\cdot}Al_2(SO_4)_3{\cdot}22H_2O$ is 44.44%. The experimentally determined result and the theoretical value are in good agreement.

Steps 5, 6, 7 and 8 temperatures of 612 and 640 °C.

In contrast to the thermal decomposition of the other halotrichites studied in this work one sharp DTG peak is observed at 612 with a second peak at 640 °C. The mass losses at these two temperatures are 22.69 and 4.55%. The theoretical mass loss for wupatkiite is 35.91%. The ion current curves for evolved SO_2 show maxima at 614 and 640 °C. These two temperatures are supported by the ion current curves for O_2 where another ion current SO_2 peak is observed at 570 °C; a small DTG peak is observed at this temperature.

3.3. Comparison with paragenically related minerals

A comparison may be made with jarosites [48–53]. Mass loss steps of K jarosite occur over the 130–330 and 500–622 °C temperature range and are attributed to dehydroxylation and

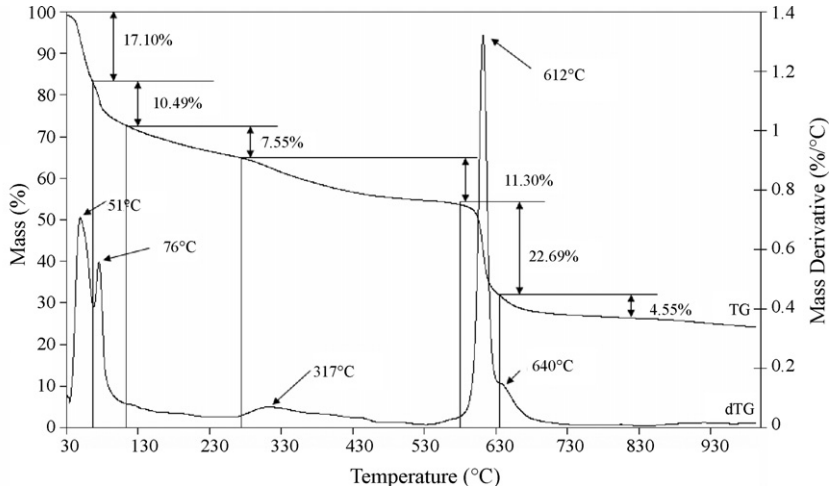

Fig. 8. TG and DTG of wupatkiite.

desulphation. The thermal decomposition of Na-jarosite shows three mass loss steps at 215–230, 316–352 and 555–595 °C. For Pb-jarosite two mass loss steps associated with dehydroxylation are observed at 390 and 418 °C and a third mass loss step at 531 °C is attributed to the loss of SO_3. For argentjarosite, dehydroxylation occurs in three stages at 228, 383, 463 °C with the loss of 2, 3 and 1 hydroxyl units. Loss of sulphate occurs at 548 °C and is associated with a loss of oxygen. At 790 °C loss of oxygen only leaves metallic silver and hematite.

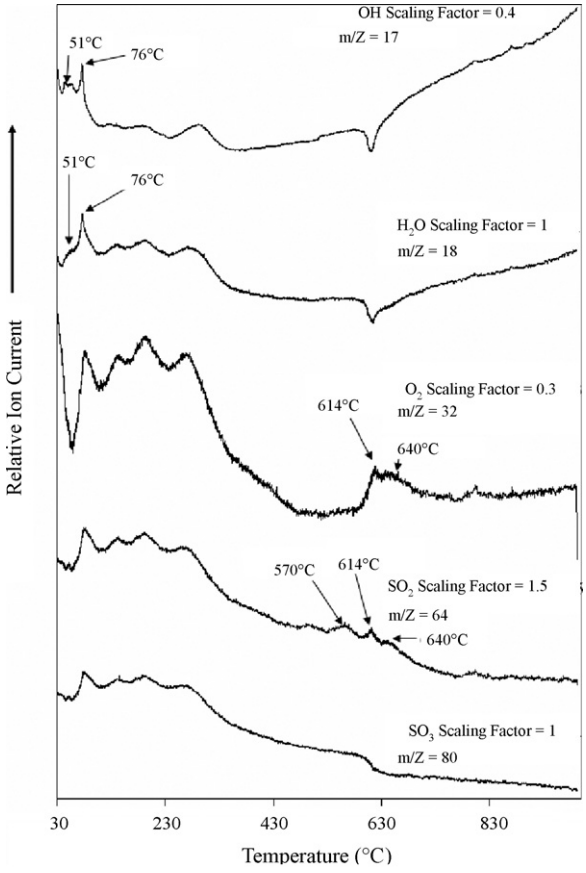

Fig. 9. Evolved gas analysis for wupatkiite.

The decomposition steps for lead jarosite (as an example of jarosites) may be given as:

Step 1 Temperature 390 °C

$$PbFe_6(SO_4)_4(OH)_{12} \rightarrow PbO_2Fe_6(SO_4)_4(OH)_8 + 2H_2O$$

Step 2 Temperature 418 °C

$$PbO_2Fe_6(SO_4)_4(OH)_8 \rightarrow PbO_6Fe_6(SO_4)_4 + 4H_2O$$

Step 3 Temperature 531 °C

$$PbO_6Fe_6(SO_4)_4 \rightarrow PbSO_4 + 3SO_3 + 3Fe_2O_3$$

Step 4 Temperature 759 °C

$$PbSO_4 \rightarrow PbO + SO_3$$

An early study using TGA methods showed that the plumbojarosite decomposed at 500 °C [17]. Another study suggested that the jarosite was completely dehydrated by 450 °C [54]. It was found that at temperatures above 550 °C further decomposition occurred with the loss of water and sulphur trioxide [54]. The thermal decomposition was complete by 950 °C. The final products were a mixture of hematite and PbO [54].

It is obvious that the halotrichites decompose at significantly higher temperatures than jarosites.

Evaporite minerals such as are found in the El Jaroso Ravine, Sierra Almagrera, Spain include halotrichites and jarosites as well as the sulphates of Fe, K, Ca and others. The importance of halotrichite and jarosite formation and its decomposition depends upon its presence in mine tailings, soils, sediments and evaporite deposits [55]. These types of deposits form in acid soils where the pH is less than 3.0 pH units [56]. Such acidification results from the oxidation of pyrite which may be from bacterial action or through air-oxidation. The Mars mission rover known as *Opportunity* has been used to discover the presence

of jarosite on Mars, thus providing evidence for the existence or pre-existence of water on Mars. Interest in evaporite minerals and their thermal stability rests with the possible identification of these minerals and related dehydrated paragenetically related minerals on planets. The existence of these minerals on planets would give a positive indication of the existence or at least pre-existence of water on Mars. Further such minerals are formed through crystallization from solutions.

4. Conclusions

Thermogravimetric and differential analysis of mineral known as pseudoalums including halotrichites, apjohnite, pickeringite and wupatkiite. EDX analysis shows the chemical formula of the minerals to be $(Fe_{0.75}^{2+},Mg_{0.25})SO_4{\cdot}Al_2(SO_4)_3{\cdot}22H_2O$,$(Mn_{0.64}^{2+},Mg_{0.28},Zn_{0.08})SO_4{\cdot}Al_2(SO_4)_3{\cdot}22H_2O$, $(Fe_{0.22}^{2+},Mg_{0.78})SO_4{\cdot}Al_2(SO_4)_3{\cdot}22H_2O$, $(Co_{0.45},Fe_{0.55}^{2+})SO_4{\cdot}Al_2(SO_4)_3{\cdot}22H_2O$, respectively. X-ray diffraction showed the minerals to be phase pure except for pickingerite which showed the presence of gypsum.

The halotrichite minerals showed in general three low temperature thermal decomposition steps attributed to dehydration. A fourth dehydration step at around 317 °C was observed and was assigned to water trapped within the halotrichite structure. Depending on the halotrichite 2, 3 or 4 higher temperature thermal decomposition steps are observed. For halotrichite thermal decomposition steps are observed at 546, 625, 697 and 738 °C and are attributed to the decomposition of sulphate anions to SO_3 and consequentially to SO_2 and $1/2O_2$. A comparison with the thermal decomposition of jarosites shows that the halotrichites decompose at higher temperatures.

Acknowledgments

The financial and infrastructure support of the Queensland University of Technology Inorganic Materials Research Program of the School of Physical and Chemical Sciences is gratefully acknowledged. The Australian Research Council (ARC) is thanked for funding Thermal Analysis Facilty.

References

[1] J. Sebor, Sbornik Klubu prirodovedeckeho, Prag II (1913) 2.
[2] R.M. Caven, T.C. Mitchell, J. Chem. Soc., Trans. 127 (1925) 527.
[3] H.M.E. Schurmann, Neues Jahrb. Mineral. Geol., Beil.-Bd. 66A (1933) 425.
[4] G.S. Baur, L.B. Sand, Am. Mineral. 42 (1957) 676.
[5] I. Velinov, S. Aslanyan, L. Punev, M. Velinova, Izvestiya na Geologicheskiya Institut, Bulgarska Akademiya na Naukite, vol. 19, Seriya Geokhimiya, Mineralogiya i Petrografiya, 1970, p. 243.
[6] R.D. Cody, D.L. Biggs, Can. Mineral. 11 (1973) 958.
[7] R.L. Frost, M.L. Weier, J.T. Kloprogge, F. Rull, J. Martinez-Frias, Spectrochim. Acta, Part A: Mol. Biomol. Spectrosc. 62A (2005) 176.
[8] R.L. Frost, D.L. Wain, B.J. Reddy, W. Martens, J. Martinez-Frias, F. Rull, J. Near Infrared Spectrosc. 14 (2006) 167.
[9] R.L. Frost, M. Weier, J. Martinez-Frias, F. Rull, B. Jagannadha Reddy, Spectrochim. Acta, Part A: Mol. Biomol. Spectrosc. 66 (2007) 177.
[10] S.A. Williams, F.P. Cesbron, Mineral. Mag. 59 (1995) 553.
[11] S. Menchetti, C. Sabelli, Mineral. Mag. 40 (1976) 599.
[12] P. Ballirano, F. Bellatreccia, O. Grubessi, Eur. J. Mineral. 15 (2003) 1043.
[13] P. Ballirano, Eur. J. Mineral. 18 (2006) 463.
[14] I. Krstanovic, R. Dimitrijevic, P. Ilic, Glasnik Prirodnjackog Muzeja u Beogradu, Serija A: Mineralogija, vol. 27, Geologija, Paleontologija, 1972, p. 11.
[15] S. Quartieri, M. Triscari, A. Viani, Eur. J. Mineral. 12 (2000) 1131.
[16] S. Nagai, N. Yamanouchi, Nippon Kagaku Kaishi 52 (1949) 83 (1921-47).
[17] J.L. Kulp, H.H. Adler, Am. J. Sci. 248 (1950) 475.
[18] G. Cocco, Periodico di Mineralogia 21 (1952) 103.
[19] A.I. Tsvetkov, E.P. Val'yashikhina, Doklady Akademii Nauk SSSR 89 (1953) 1079.
[20] A.I. Tsvetkov, E.P. Val'yashikhina, Doklady Akademii Nauk SSSR 93 (1953) 343.
[21] M.S.R. Swamy, T.P. Prasad, B.R. Sant, J. Therm. Anal. 16 (1979) 471.
[22] M.S.R. Swamy, T.P. Prasad, B.R. Sant, J. Therm. Anal. 15 (1979) 307.
[23] S. Bhattacharyya, S.N. Bhattacharyya, J. Chem. Eng. Data 24 (1979) 93.
[24] M.S.R. Swami, T.P. Prasad, J. Therm. Anal. 19 (1980) 297.
[25] M.S.R. Swamy, T.P. Prasad, J. Therm. Anal. 20 (1981) 107.
[26] A.C. Banerjee, S. Sood, Therm. Anal., Proc. Int. Conf., 7th, vol. 1, 1982, p. 769.
[27] J.E. Dutrizac, J.L. Jambor, Chapter 8 Jarosites and their application in hydrometallurgy, 2000, p. 405.
[28] P.S. Thomas, D. Hirschausen, R.E. White, J.P. Guerbois, A.S. Ray, J. Therm. Anal. Calorim. 72 (2003) 769.
[29] R.L. Frost, K.L. Erickson, J. Therm. Anal. Calorim. 76 (2004) 217.
[30] R.L. Frost, K. Erickson, M. Weier, J. Therm. Anal. Calorim. 77 (2004) 851.
[31] R.L. Frost, M.L. Weier, K.L. Erickson, J. Therm. Anal. Calorim. 76 (2004) 1025.
[32] R.L. Frost, M.L. Weier, J. Therm. Anal. Calorim. 75 (2004) 277.
[33] R.L. Frost, W. Martens, Z. Ding, J.T. Kloprogge, J. Therm. Anal. Calorim. 71 (2003) 429.
[34] R.L. Frost, Z. Ding, H.D. Ruan, J. Therm. Anal. Calorim. 71 (2003) 783.
[35] R.L. Frost, S.J. Palmer, J.M. Bouzaid, B.J. Reddy, J. Raman Spectrosc. 38 (2007) 68.
[36] R.L. Frost, D.A. Henry, M.L. Weier, W. Martens, J. Raman Spectrosc. 37 (2006) 722.
[37] R.L. Frost, A.W. Musumeci, J.T. Kloprogge, M.O. Adebajo, W.N. Martens, J. Raman Spectrosc. 37 (2006) 733.
[38] R.L. Frost, J. Cejka, M. Weier, W.N. Martens, J. Raman Spectrosc. 37 (2006) 879.
[39] R.L. Frost, M.L. Weier, J. Cejka, J.T. Kloprogge, J. Raman Spectrosc. 37 (2006) 585.
[40] R.L. Frost, J. Cejka, M.L. Weier, W. Martens, J. Raman Spectrosc. 37 (2006) 538.
[41] R.L. Frost, M.L. Weier, B.J. Reddy, J. Cejka, J. Raman Spectrosc. 37 (2006) 816.
[42] R.L. Frost, M.L. Weier, W.N. Martens, J.T. Kloprogge, J. Kristof, J. Raman Spectrosc. 36 (2005) 797.
[43] R.L. Frost, R.-A. Wills, M.L. Weier, W. Martens, J. Raman Spectrosc. 36 (2005) 435.
[44] S.V. Mityushov, Y.A. Lainer, V.P. Dolganyov, Izvestiya Vysshikh Uchebnykh Zavedenii, Tsvetnaya Metallurgiya, 1991, p. 21.
[45] V.P. Ivanova, E.L. Rozinova, T.P. Nikitina, Konstitutsiya i Svoistva Mineralov 8 (1974) 81.
[46] V.P. Ivanova, Zapiski Vserossiiskogo Mineralogicheskogo Obshchestva 90 (1961) 50.
[47] S.L. Reddy, G.S. Reddy, D.L. Wain, W.N. Martens, B.J. Reddy, R.L. Frost, Spectrochim. Acta, Part A 65A (2006) 1227.
[48] R.L. Frost, R.-A. Wills, M.L. Weier, A.W. Musumeci, W. Martens, Thermochim. Acta 432 (2005) 30.
[49] R.L. Frost, M.L. Weier, W. Martens, J. Therm. Anal. Calorim. 82 (2005) 115.
[50] R.L. Frost, R.-A. Wills, M.L. Weier, W. Martens, Thermochim. Acta 437 (2005) 30.

[51] R.L. Frost, R.-A. Wills, J.T. Kloprogge, W. Martens, J. Therm. Anal. Calorim. 84 (2006) 489.
[52] R.L. Frost, R.-A. Wills, J.T. Kloprogge, W.N. Martens, J. Therm. Anal. Calorim. 83 (2006) 213.
[53] L. Frost Ray, L. Weier Matt, W. Martens, S. Mills, Spectrochim. Acta. Part A, Mol. Biomol. Spectrosc. 63 (2006) 282.
[54] T. Taberdar, H. Gulensoy, A.O. Aydin, Marmara Universitesi Fen Bilimleri Dergisi 2 (1985) 76.
[55] T. Buckby, S. Black, M.L. Coleman, M.E. Hodson, Mineral. Mag. 67 (2003) 263.
[56] P.A. Williams, Oxide Zone Geochemistry, Ellis Horwood Ltd., Chichester, West Sussex, England, 1990.